# Melting of Secondary-Phase Particles in Al-Mg-Si Alloys

ODDVIN REISO, NILS RYUM, and JAN STRID

The melting of secondary-phase particles—or, more precisely, the melting of such particles together with the surrounding matrix—in two ternary Al-Mg-Si alloys has been studied. In the quasi-binary Al-$Mg_2Si$ alloy, one melting reaction is found. In the alloy with an Si content in excess of that necessary to form $Mg_2Si$, three different melting reactions are observed. At upquenching temperatures above the eutectic temperature, the reaction rates are very high, and it is assumed that they are controlled by diffusion of the alloying elements in the liquid. Melting is also observed after prolonged annealing at temperatures below the eutectic temperature in these alloys, which is explained by the different diffusion rates of Mg and Si. The rate of the melting reaction is in this case assumed to be controlled by diffusion of the alloying elements in the solid $\alpha$-Al phase. It is shown that calculation of the particle/matrix interface composition, which determines when melting is possible, cannot be made solely on the basis of the phase diagram, but must also include the rate of diffusion of Mg and Si. The melting temperatures observed differ somewhat from the accepted eutectic temperatures for these alloys. On prolonged annealing, the liquid droplets formed dissolve into the surrounding matrix and their chemical composition is found to change during dissolution. The resulting eutectic structure after quenching of a droplet is explained by the phase diagram and the different diffusion rates of Mg and Si as well as by the nucleation conditions of the constituents involved.

## I. INTRODUCTION

HOMOGENIZATION heat treatment of alloys is a process of great industrial importance. Usually it is carried out on castings in order to improve the properties of the casting or to facilitate subsequent processing steps to final products. In such cases, the homogenization treatment is carried out as a well-defined operation with rather strict temperature control.

A similar process often takes place during hot deformation, such as extrusion, rolling, and forging, where generally a multiphase alloy is plastically deformed in the single-phase region. Homogenization then takes place during the heating period and during the deformation process. In these cases, the homogenization reaction is much less accurately controlled.

One problem associated with the homogenization process is incipient melting. If the composition of a binary alloy is higher than $C_{max}$ (Figure 1) and the alloy is annealed at a temperature higher than $T_{eut}$, the alloy starts to melt. The plastic deformation of an alloy in this condition is problematic due to low ductility, but the phenomenon may also be utilized—for example, during thixocasting.

In alloys with segregation of the alloying elements, the composition may locally exceed the critical composition $C_{max}$, even though the mean composition is lower. Also in this case, incipient melting occurs when $T$ is higher than $T_{eut}$, but this is a transient phenomenon.

Recent experiments[1–5] have demonstrated that incipient melting may take place during homogenization heat treatment of aluminum alloys even when the alloy is close to equilibrium at a low temperature and the mean, as well as the local matrix concentration of the alloy, is far below $C_{max}$. Reiso[1,2] arrived at this conclusion in a rather indirect way by investigating the extrudability of several aluminum alloys. It was shown that one of the limiting conditions for extrusion speed probably is incipient melting of secondary phases, and it was indicated that the most likely reaction was the formation of a liquid of eutectic composition. Similar results were also obtained by Gjestland *et al.*[3]

Lohne and Ryum[4] subsequently studied the binary alloy Al-Si at mean compositions below $C_{max}$ and clearly demonstrated that local melting occurred in this alloy when the annealing temperature was higher than $T_{eut}$. The incipient melting reaction of secondary phases was further studied by Reiso *et al.*[5] in a binary Al-Cu alloy, where a more detailed characterization of the reaction is given.

In the present investigation, the study of this incipient melting reaction is extended to ternary Al-Mg-Si alloys. This alloy system is of great industrial importance—for example, in the extrusion industry, where it is the major Al alloy system tonnagewise.* In the present investigation, these melting reactions are studied in more detail.

*Reiso[6] has previously shown that incipient melting occurs in these alloys.

## II. EXPERIMENTAL

Two Al-Mg-Si alloys were produced by directional solidification. The chemical compositions of the alloys were carefully determined by spectrographic analysis and are given in Table I. The alloys were made from high-purity Al, and the amount of any impurity element was less than 0.01 wt pct. Alloy 1 is a quasi-binary Al-$Mg_2Si$ alloy, while alloy 2 has a Si content in excess of that necessary to form $Mg_2Si$.

ODDVIN REISO, Senior Research Metallurgist, and JAN STRID, Senior Research Metallurgist, are with the Metallurgical R & D Centre, Hydro Aluminium a.s, N-6600 Sunndalsøra, Norway. NILS RYUM, Professor, is with the Division of Metallurgy, The Norwegian Institute of Technology, University of Trondheim, NTH, 7034 Trondheim, Norway.

Manuscript submitted September 22, 1992.

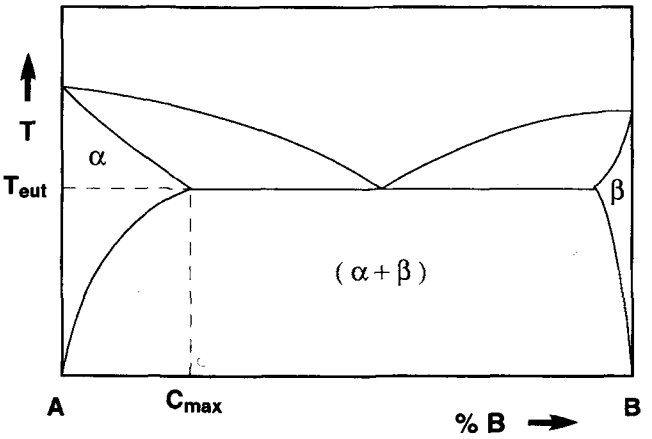


Fig. 1—Schematic eutectic binary phase diagram.

**Table I. Chemical Compositions of the Alloys, Weight Percent**

| Alloy No. | Composition (Wt Pct) | | | |
|---|---|---|---|---|
| | Mg | Si | $Mg_2Si$ | ΔSi* |
| 1 | 0.57 | 0.33 | 0.90 | — |
| 2 | 0.60 | 0.70 | 0.95 | 0.35 |

*Si content in excess of that necessary to form $Mg_2Si$.

The castings, approximately 2 kg each, were homogenized for 24 hours at 540 °C, cold-rolled with intermediate annealing at 540 °C, and cut to specimens 25 × 25 × 2.5 $mm^3$ in size. To obtain a uniform distribution of coarse $Mg_2Si$ and Si particles and an equilibrium matrix composition, the samples were first annealed at 540 °C for 1 hour in air and subsequently cooled at a rate of 1 °C/h down to 100 °C.

The incipient melting reactions were studied by upquenching the specimens in a salt bath to various temperatures and then isothermally annealing the specimens at the upquench temperature for different periods of time. The temperature was measured using thermocouples inserted into holes drilled in the samples parallel to their broad face. The thermocouple and temperature-registration equipment used was checked against standardized and calibrated temperature-measurement equipment. The accuracy of the thermocouple and equipment used was found to be better than ±0.5 °C. The temperature stability during heat treatment in the salt bath was better than ±1 °C. After these heat treatments, the specimens were cooled in air. The rate of solidification of the liquid droplets that formed was then such that the resulting eutectic had an internal structure which could be resolved in the light microscope.

In addition to this heat-treatment procedure, samples of alloy 2 were brought close to equilibrium at a higher temperature prior to upquenching in the salt bath in order to study the effect of a different matrix composition on the melting reaction. This was done by annealing the homogenized and slowly cooled samples for 19 days at 500 °C.

Metallographic examinations were performed in the light microscope on unetched specimens. The different phases ($Mg_2Si$, Si, and α-Al) were identified by their color and shape. This correspondence was established by a combination of light and scanning microscopy. The chemical compositions were determined in the scanning electron microscope (SEM) equipped with a wavelength-dispersive spectrometer (WDS) and an energy-dispersive spectrometer (EDS). Measurements were done on unetched specimens. Care was taken to avoid the introduction of water during polishing, because $Mg_2Si$ particles react rapidly with traces of water. Reliable quantitative analysis of individual particles could be obtained when the particles were larger than approximately 2 μm. The accelerating voltage was 8 kV with a beam current of approximately 2 nA. Often the eutectics formed were very finely dispersed, and quantitative chemical analysis from the individual particles in the eutectics was impossible. In such cases, the type of eutectic (binary or ternary) could be determined by a combination of light microscopy, by which the types of phase particles could be determined as explained above, and measurement of the mean chemical composition of the eutectic in the SEM.

## III. RESULTS

The microstructures of the alloys after slow cooling (prior to upquenching) are shown in Figures 2(a) and (b). As expected, only $Mg_2Si$ particles were found in the quasi-binary alloy (alloy 1, Figure 2(a)). These had a bulky shape and were situated on the grain boundaries or in the interior of the grains. In alloy 2, coarse $Mg_2Si$ particles were also found at the grain boundaries and in the interior of the grains, but in addition some Si particles were found (Figure 2(b)). Most of these Si particles were located on the grain boundaries, frequently in contact with an $Mg_2Si$ particle, but a few were also found in the interior of the grains. "Free" $Mg_2Si$ and Si particles (*i.e.*, these two particles were not in contact with each other) were also found. The $Mg_2Si$ particles were somewhat larger in alloy 2 than in alloy 1.

A typical temperature/time profile recorded by the thermocouple during upquenching is shown in Figure 3. As can be seen, the temperature increased steeply during the first seconds in the salt bath and reached a temperature approximately 2 °C below the set point after about 15 seconds. The last 2 degrees were approached more slowly, and the desired temperature was reached after approximately 20 seconds.

After upquenching and cooling in air, only one melting reaction was identified in alloy 1. The $Mg_2Si$ particles, together with the surrounding matrix, melted and formed a binary eutectic structure upon solidification that consisted of $Mg_2Si$ and α-Al. In order for this reaction to occur after ~0 second annealing time (*i.e.*, upquenching to temperature and cooling in air immediately as the desired temperature was reached), the temperature had to be increased to 593 °C. (Annealing of individual samples was done at 1 °C intervals in the range of 590 °C to 600 °C.) An example of this reaction is presented in Figure 4, which shows the structure in alloy 1 after ~0 second annealing time at 593 °C.

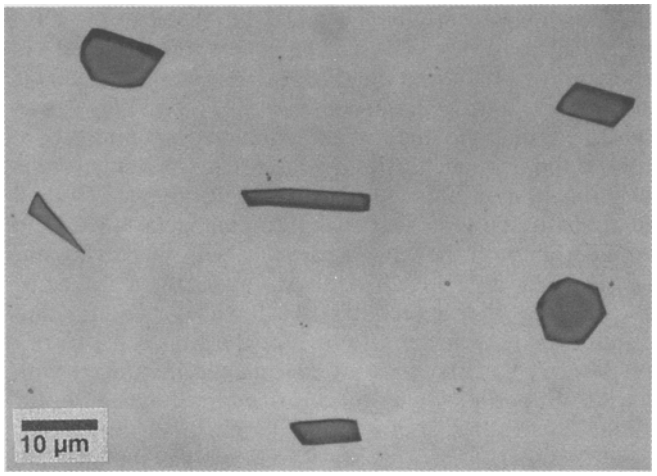


(*a*)

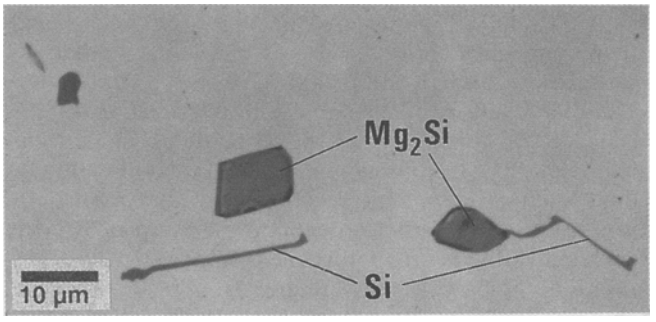


(*b*)

Fig. 2—Microstructures (light microscopy) of the alloys after slow cooling: (*a*) $Mg_2Si$ particles in alloy 1; and (*b*) $Mg_2Si$ and Si particles in alloy 2.

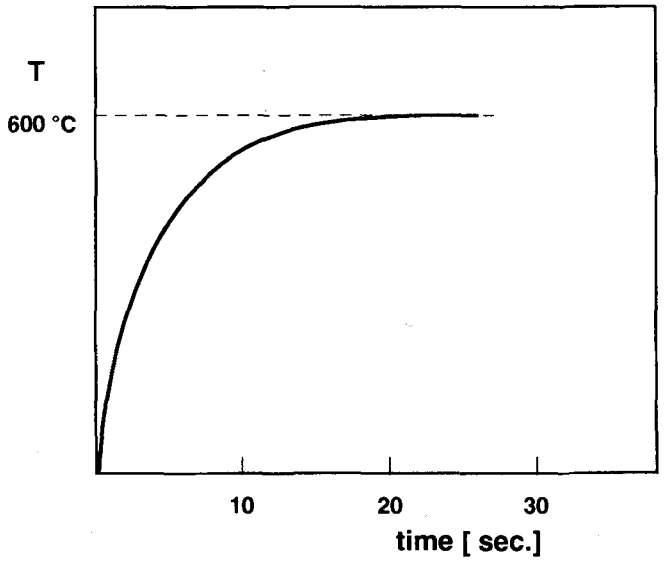


Fig. 3—Temperature/time profile of a specimen during upquenching to 600 °C.

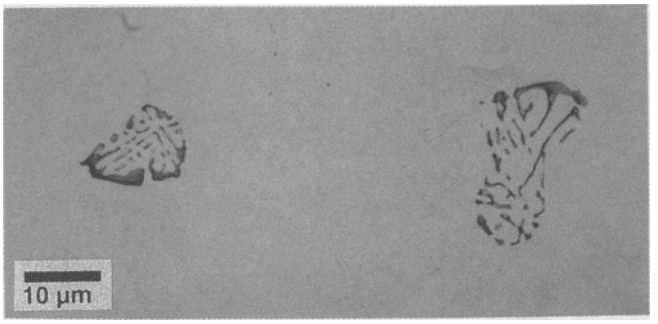


Fig. 4—Eutectic microstructure (Al-$Mg_2Si$, light microscopy) in alloy 1 formed during upquenching to 593 °C, followed by quenching in air (~0 s annealing time).

In alloy 2, several reactions were observed. After upquenching to 560 °C, a reaction was found where $\alpha$-Al, $Mg_2Si$, and Si particles in contact with one another melted and on subsequent solidification formed a ternary eutectic. Figure 5(a) shows an example of this reaction after upquenching to 560 °C and cooling in air immediately (*i.e.*, no annealing time). Analysis by EDS in the SEM in combination with light microscopy showed this eutectic to consist of $\alpha$-Al, $Mg_2Si$, and Si. In order to identify the exact temperature for this ternary eutectic reaction, annealing was carried out at 1 °C intervals from 555 °C to 560 °C. Even after long annealing times (60 seconds), the temperature had to be increased to 560 °C before the reaction occurred. At 560 °C, the reaction occurred spontaneously (*i.e.*, ~0 second annealing time). This ternary eutectic was found primarily on the grain boundaries, and its pointed shape may indicate that the grain boundaries are wetted by the melt (Figure 5(a)).

A second reaction in alloy 2 occurred spontaneously after upquenching to 577 °C (Figure 5(b)). Here the Si particles not in contact with any $Mg_2Si$ particles (free Si particles) melted and on subsequent solidification formed a binary eutectic consisting of $\alpha$-Al and Si. The exact melting temperature was difficult to determine, as these free Si particles were rather scarce and were not observed in all samples. The reaction, however, was observed in samples at temperatures down to 573 °C with ~0 second annealing time after upquenching.

A third reaction in alloy 2 was found in samples upquenched to higher temperatures than the melting temperatures for the two reactions already described. This is the same reaction as found in alloy 1, where the free $Mg_2Si$ particles and $\alpha$-Al melt and on subsequent solidification form a eutectic consisting of $\alpha$-Al and $Mg_2Si$. Figure 5(c) shows an example of the structure formed on upquenching to 593 °C followed by cooling. Just as for alloy 1, the samples had to be upquenched to 593 °C or above for this reaction to occur spontaneously.

Several interesting observations were made concerning the reaction between $\alpha$-Al and $Mg_2Si$ in alloys 1 and 2. First, it was observed that in samples that had been annealed at 600 °C for longer periods of time, the Al-$Mg_2Si$ melt separated into two types of eutectics on subsequent solidification. After ~0 second annealing time, mainly the binary Al-$Mg_2Si$ eutectic was found (as also observed in Figure 6(a), as well as Figures 4 and 5(c)). However, as the annealing time at 600 °C was

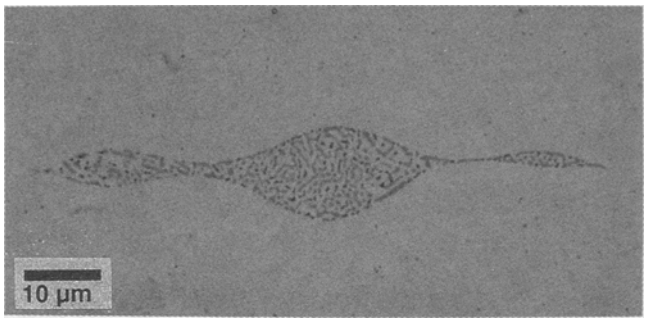


(*a*)

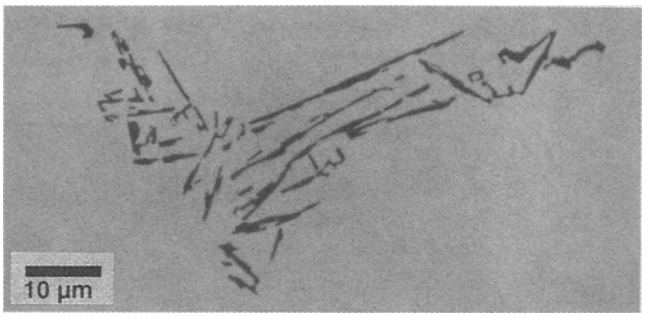


(*b*)


(*c*)

Fig. 5—Microstructures (light microscopy) in alloy 2 after upquenching and subsequent cooling in air: (*a*) Ternary Al-$Mg_2Si$-Si eutectic after upquenching to 560 °C with ~0 s annealing time before cooling; (*b*) binary Al-Si eutectic after upquenching to 577 °C with ~0 s annealing time; and (*c*) Al-$Mg_2Si$ eutectic upquenching to 593 °C with ~0 s annealing time.

increased, a second eutectic was observed in connection with the Al-$Mg_2Si$ eutectic. Light microscopy in combination with EDS analysis in the SEM showed this second eutectic to be the ternary Al-$Mg_2Si$-Si eutectic. At increasing annealing time, the amount of this ternary eutectic increased relative to the amount of the binary eutectic, and after approximately 5 to 10 minutes of annealing time, mainly the ternary eutectic was present in alloy 2. Figures 6(a) through (d) show the structure in alloy 2 after annealing at 600 °C for approximately 0, 20, 60, and 600 seconds, respectively. (Note the decreasing size of the eutectics with increasing annealing time.) Similar observations also were made for this reaction in alloy 1.

A second observation concerning the reaction between $\alpha$-Al and $Mg_2Si$ in alloys 1 and 2 is related to the temperature and time for this melting reaction to occur. As shown previously, the melting reaction was spontaneous at 593 °C. During upquenching to $T < 593$ °C, it was observed that the melting reaction started after some time at the upquenching temperature. An example of this phenomenon in alloy 2 is illustrated in Figures 7(b) and (c), which show an increasing amount of a eutectic in connection with the $Mg_2Si$ particles with increasing annealing time at 590 °C. Analysis by EDS in the SEM showed that this apparently is a binary Al-Si eutectic. (Notice also the faceted shaped of the $Mg_2Si$ particles.) At 590 °C, the first trace of the eutectic in contact with the $Mg_2Si$ particles was not observed until annealing for about 20 to 40 seconds. After longer annealing times (~2 minutes), the entire $Mg_2Si$ particle has melted, and light microscopy together with EDS analysis indicates that a mixture of Al-$Mg_2Si$ eutectic and a ternary Al-$Mg_2Si$-Si eutectic or only a ternary Al-$Mg_2Si$-Si eutectic is left (Figures 7(d) and (e), 590 °C, 5 and 10 minute annealing time, respectively; similar to Figures 6(b) through (d) at 600 °C).

Similar results were also obtained by annealing alloy 1 at 590 °C. In this case, the $Mg_2Si$ particles and the eutectic melt dissolved much more quickly than in alloy 2. Good micrographs of the reaction were difficult to obtain, because the particles containing these phases were very small. The start of this melting reaction was observed at as low a temperature as 580 °C after an 8 minute annealing time in alloy 2. It should be noted that this is 15 °C below the accepted eutectic temperature in the quasi-binary Al-$Mg_2Si$ alloy system.[7,8]

In order to study the effect of a different matrix composition prior to upquenching on the melting reaction of $Mg_2Si$ and Al, samples of alloy 2 were brought close to equilibrium at a higher temperature. This was done by annealing the homogenized and slowly cooled samples for 19 days at 500 °C. These samples contained only $Mg_2Si$-phase particles.

It was also found for these samples that the upquenching temperature at which the $Mg_2Si$ particles and the surrounding matrix melted completely after ~0 second annealing time was 593 °C. By upquenching these samples to a temperature lower than the quasi-binary eutectic temperature, the first appearance of a eutectic in connection with the $Mg_2Si$ particles was observed even after ~0 second annealing time at 590 °C.

## IV. DISCUSSION

In a previous investigation of the dissolution and local melting of $Al_2Cu$ particles in the binary Al-4.2 wt pct Cu alloy, the observations could be explained in a consistent way by assuming local equilibrium at the matrix/particle interface during upquenching. When the upquenching temperature was known, the concentration at the interface was also known, and the kinetics of the dissolution and melting reaction could be described in a fairly simple way by solving the diffusion equation with the appropriate boundary conditions.[5]

In the ternary Al-Mg-Si alloy system, the experimental observations are somewhat more complicated. In the

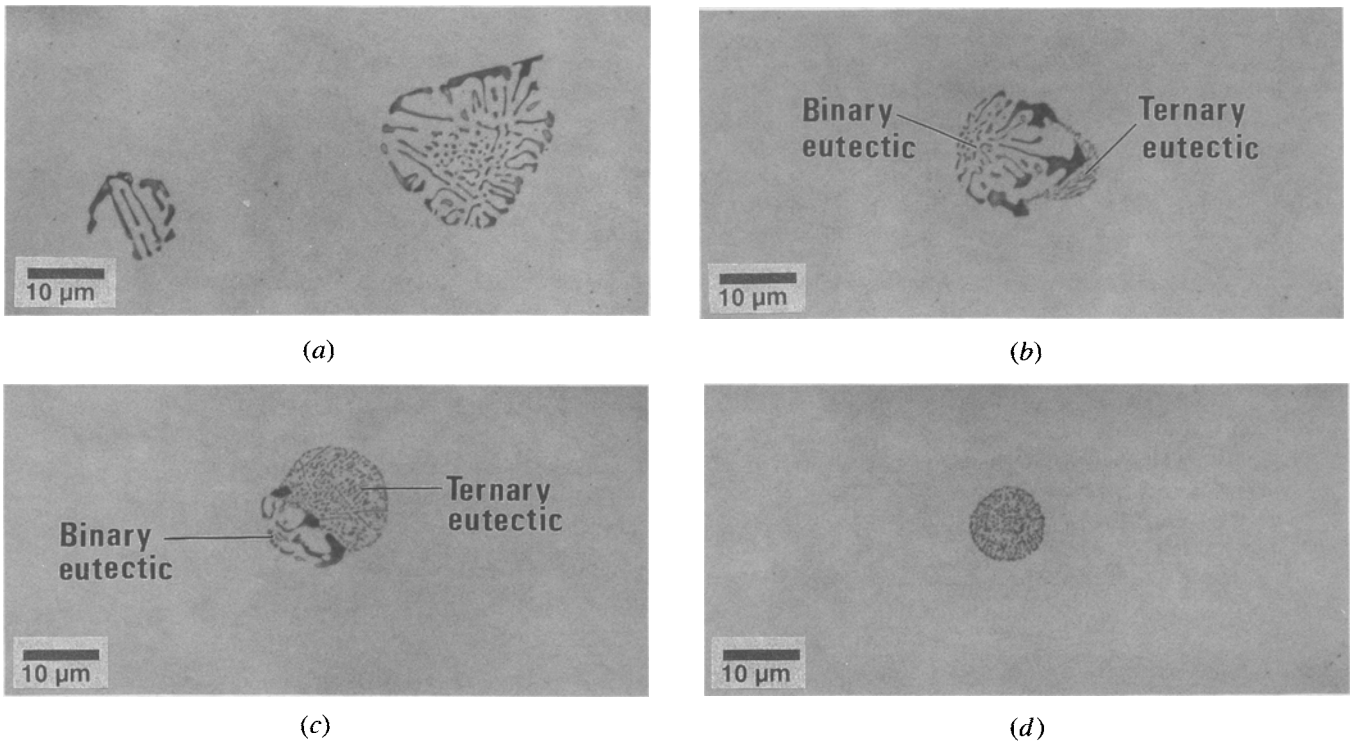


Fig. 6—Changes in the microstructure (light microscopy) in alloy 2 with increasing annealing times at 600 °C before cooling in air. (Melting reaction: $\alpha$-Al + $Mg_2Si \rightarrow$ liq.) Note the increasing amount of the ternary Al-$Mg_2Si$-Si eutectic by increasing time: (*a*) ~0 s (binary Al-$Mg_2Si$-eutectic); (*b*) 20 s; (*c*) 60 s; and (*d*) 600 s (only ternary eutectic).

quasi-binary Al-$Mg_2Si$ alloy, local melting is observed even at temperatures markedly below the eutectic temperature of 595 °C.[7,8] It is also observed that melting at such temperatures does not occur immediately, but after a certain period of annealing time. The chemical composition of the liquid droplet formed during this reaction (Al + $Mg_2Si \rightarrow$ liq) is found to change with annealing time. In the alloy on the Si-rich side of the quasi-binary section, two more local melting reactions are observed in addition to that found in the quasi-binary alloy.

The remainder of this discussion has been divided into three parts, one for each of the different melting reactions as follows:

A. $\alpha$-Al + $Mg_2Si \rightarrow$ liq (alloys 1 and 2)
   1. $T > T_{eut}$
   2. $T < T_{eut}$
B. $\alpha$-Al + Si $\rightarrow$ liq (alloy 2)
C. $\alpha$-Al + $Mg_2Si$ + Si $\rightarrow$ liq (alloy 2)

### A. *$\alpha$-Al + $Mg_2Si \rightarrow$ liq (Alloys 1 and 2)*

Whereas the growth of a precipitate in a supersaturated ternary matrix has been investigated in detail,[9] the reverse reaction—namely, the dissolution of a particle in such an alloy—seems to have been somewhat ignored. Coates[9] showed that when the growth rate, $v$, of the particles can be written as $v = k(1/\sqrt{t})$ ($k$ is constant), the concentration at the interface will not change with time. Coates restricted his study to particles that are shape-conserving during growth. For such particles, the growth rate always satisfies the preceding requirement.

On the other hand, the dissolution rate of a particle during the dissolution process does not satisfy this requirement, except after long dissolution times.[10] If it is assumed, as was done in the analysis of the corresponding reaction in the binary Al-Cu alloy,[5] that local equilibrium is maintained during upquenching of a ternary alloy as well, the concentrations at the interface are not given by the phase diagram alone. The rates of diffusion of the two alloying elements must also be included in the determination of these concentrations.

The quasi-binary alloy (alloy 1) will be considered first. The alloy is brought close to equilibrium at a low temperature, $T_L$, and is then upquenched to a higher temperature, $T_H$. It is assumed that local equilibrium is maintained at the $\alpha$-Al/$Mg_2Si$ interface and that dissolution of the $\beta$-$Mg_2Si$ particles is controlled by diffusion in the $\alpha$-Al phase. The composition $C^i_{Mg,Si}$ at the interface at the upquenching temperature $T_H$ must now be such that mass conservation is satisfied at the interface moving at a velocity $v$. The interface concentration and the interface velocity are found by solving the two Fick's equations for the diffusion of Mg and Si atoms under such conditions. The Appendix to this article presents a calculation of the kinetics of this particle dissolution.

From the Appendix, the ratio between the Mg and Si matrix concentrations at the interface ($C^i_{Mg}$ and $C^i_{Si}$) is given by

$$\frac{C^i_{Mg} - C^\infty_{Mg}}{C^i_{Si} - C^\infty_{Si}} = 2 \left( \frac{\frac{D^\alpha_{Si}}{r^*} + \sqrt{\frac{D^\alpha_{Si}}{\pi t}}}{\frac{D^\alpha_{Mg}}{r^*} + \sqrt{\frac{D^\alpha_{Mg}}{\pi t}}} \right) \quad [A5]$$

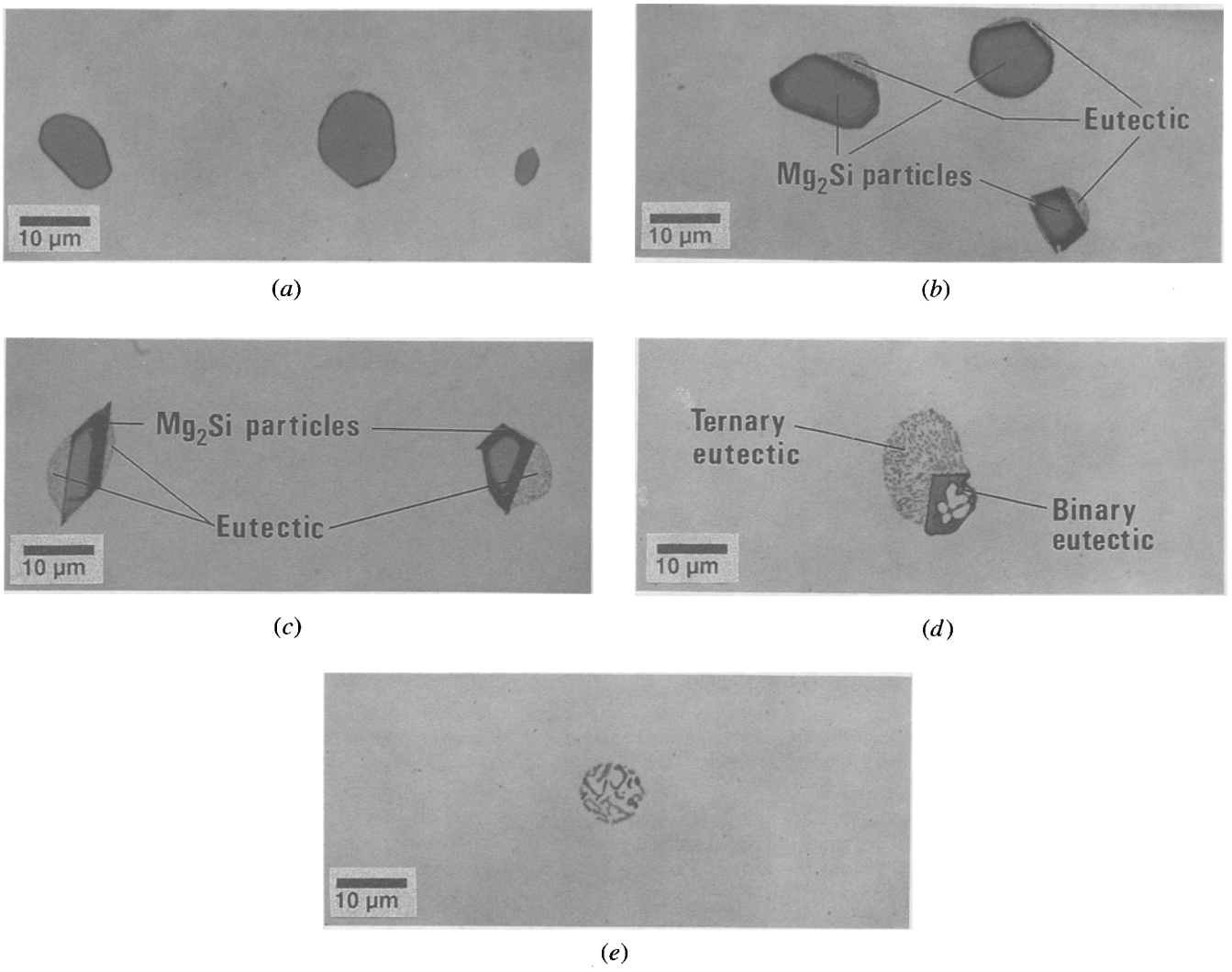


Fig. 7—Melting reaction between α-Al and $Mg_2Si$ in alloy 2 at lower than eutectic temperature after long annealing times at 590 °C prior to cooling in air: (*a*) ~0 s ($Mg_2Si$ particles, no melting); (*b*) 40 s; (*c*) 60 s; (*d*) 300 s; and (*e*) 600 s (only ternary eutectic). Light microscopy.

where $r^*$ is the position of the phase boundary $\beta/\alpha$ and is equal to the radius of the $\beta$-phase particle, $C^{\infty}_{Mg}$ and $C^{\infty}_{Si}$ are the concentrations remote from this particle, and $D^{\alpha}_{Mg}$ and $D^{\alpha}_{Si}$ are the diffusion coefficients.

There are two limiting cases. For short dissolution times,

$$\frac{C^{i}_{Mg} - C^{\infty}_{Mg}}{C^{i}_{Si} - C^{\infty}_{Si}} = 2\sqrt{\frac{D^{\alpha}_{Si}}{D^{\alpha}_{Mg}}} \qquad [A6]$$

For long dissolution times,

$$\frac{C^{i}_{Mg} - C^{\infty}_{Mg}}{C^{i}_{Si} - C^{\infty}_{Si}} = 2\left(\frac{D^{\alpha}_{Si}}{D^{\alpha}_{Mg}}\right) \qquad [A7]$$

As can be seen, the interface composition will be located along the quasi-binary line only if $D^{\alpha}_{Si} = D^{\alpha}_{Mg}$.

1. $\alpha\text{-}Al + Mg_2Si \rightarrow liq\ at\ T > T_{eut}$

The melting reaction at temperatures above the eutectic temperature of 595 °C, as given in References 7 and 8, will be considered first. Complete melting of the $Mg_2Si$-phase particles was observed after very short times at these temperatures (spontaneous melting). In fact, complete melting was observed after ~0 second holding time at upquenching temperatures of 593 °C and above. If spontaneous melting occurs at $T > T_{eut}$ (see later), a quasi-binary eutectic temperature of 593 °C as given by Fischer[11] is in better agreement with the observed results than 595 °C as given in References 7 and 8. These observations were made in both alloys, which is to be expected if the alloys have been brought to equilibrium at a low enough temperature. In this case, the matrix concentration in alloy 2 will be approximately the same as the matrix concentration in alloy 1 and close to the quasi-binary composition. Thus, in such a situation there should be no difference in behavior between an $Mg_2Si$ particle in alloy 1 and a "free" $Mg_2Si$ particle in alloy 2 upon upquenching. Figure 8 shows the solid-solubility limits in the Al-Mg-Si alloy system as given by Phillips;[7] the compositions of alloys 1 and 2 also are shown. If equilibrium has been established, the matrix compositions are seen to be approximately identical at temperatures below 300 °C.

An extended solid-solution isotherm at 600 °C has also

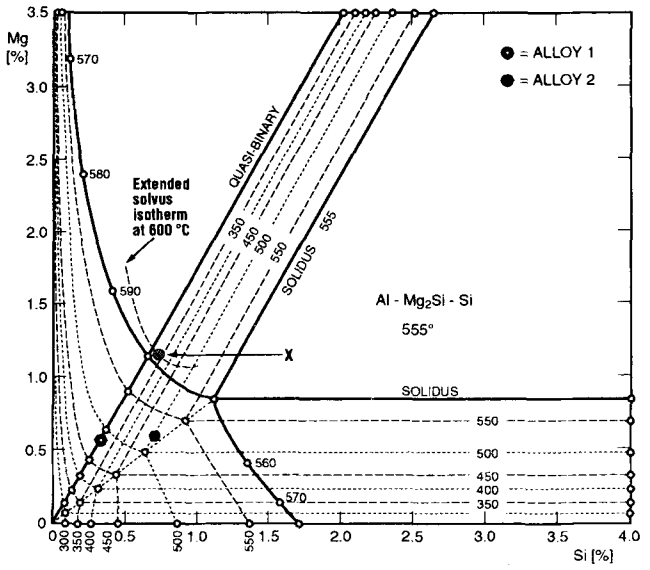


Fig. 8—Solid-solubility limits as given by Phillips.[7] The compositions of alloys 1 and 2 are indicated, as well as an extended solvus isotherm at 600 °C.

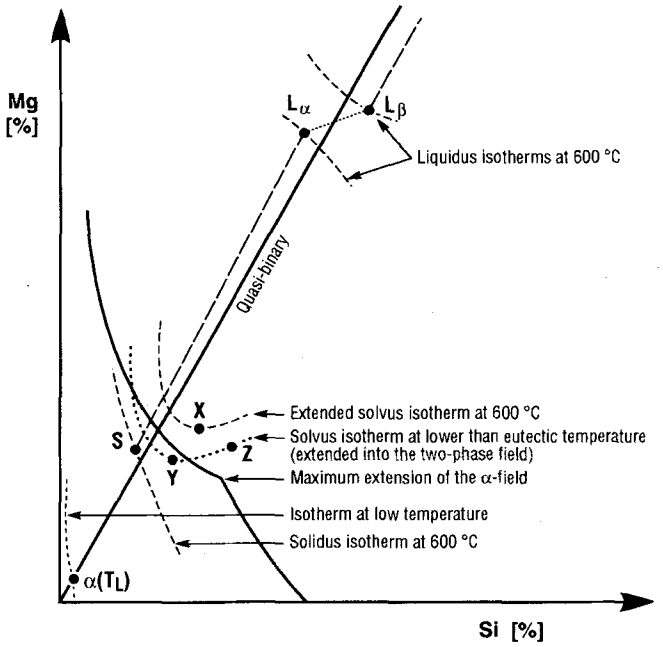


Fig. 9—Sketch of the Al-Mg-Si phase diagram. $\alpha(T_L)$ shows the location of the matrix composition before upquenching. The relevant isotherms at 600 °C are indicated (dashed lines), as are the locations of points X, S, $L_\alpha$, and $L_\beta$ at this temperature. The dotted line is a solvus isotherm at a lower temperature than the quasi-binary eutectic temperature, which has been extended into the two-phase field. The locations of points Y and Z are also shown.

been indicated in Figure 8. When upquenching to 600 °C, the matrix interface concentration will be given by Eq. [A6] on this isotherm, as indicated by point X in Figure 8. (As mentioned in the Appendix and also as given in Reference 12, $D^{\alpha}_{Mg} > D^{\alpha}_{Si}$, which gives the position of point X on the Si side of the quasi-binary line.)

As point X deviates only slightly from the quasi-binary line in Figure 8, the situation after upquenching is shown schematically on Figure 9. Immediately after upquenching, but before melting starts, the interface composition will be located on the extended solid-solution isotherm for 600 °C at point X defined by Eq. [A6]. The 600 °C isotherm is well into the liquidus field, and the condition for melting is satisfied. Matrix of composition X in equilibrium with the $\beta$-$Mg_2Si$ particle may now melt. The matrix interface in equilibrium with the melt must be located along the solidus isotherm for 600 °C, as indicated by point S in Figure 9. From the structure of the solidified droplets (*i.e.*, mainly quasi-binary Al-$Mg_2$-Si eutectic found after upquenching to 593 °C with ~0 second annealing time), it is anticipated that the mean composition of the melt in this case is rather close to the quasi-binary composition.

If it is assumed, as was done in the solid state, that the diffusion rates of Mg and Si differ in the liquid state as well, a gradient in the melt which deviates from the quasi-binary $Mg_2Si$ composition must be established during melting. Mass conservation implies that if $D^{liq}_{Mg} > D^{liq}_{Si}$, the gradient in the melt will be as shown in Figure 9, defining the point S to the left (the Mg side) of the quasi-binary composition. How much this gradient deviates from the Al-$Mg_2Si$ line in Figure 9 will be given by the difference between $D^{liq}_{Mg}$ and $D^{liq}_{Si}$. Its extreme position is a horizontal line in the diagram (*i.e.*, no gradient in Mg concentration and a maximum gradient in Si concentration) if $D^{liq}_{Mg} \gg D^{liq}_{Si}$. As long as the $Mg_2Si$-phase particle exists, local equilibrium must exist at each interface of the melt: matrix of composition S along the 600 °C solidus isotherm is free to adjust its composition in equilibrium with melt of composition $L_\alpha$ along the 600 °C liquidus isotherm, and $\beta$-$Mg_2Si$ is in equilibrium with melt of composition $L_\beta$ (Figure 9).

The bulk composition of the two solid phases involved in the melting reaction and the mean composition of the resulting liquid phase are now all located on (or very close to) a straight line in the phase diagram. This means that the melt obtains its correct composition simply by melting $\alpha$-Al and $Mg_2Si$ in the correct proportions. This reaction requires no long-range diffusion in the solid, and the reaction rate will thus be controlled by diffusion in the liquid phase. The rate of this melting reaction at $T > T_{eut}$ may thus be very high due to the high diffusion rates in the melt. This is also what was observed, and the phenomenon is referred to as a spontaneous melting reaction. It is assumed that the interface mobility does not influence the reaction rate.

As long as the $\beta$-$Mg_2Si$-phase particle exists, the composition of the melt will be restricted by the two local equilibrium conditions: $\alpha$-Al/liquid and liquid/$\beta$-$Mg_2Si$. This means that immediately after the melting reaction is complete, droplets of close-to-eutectic composition are present in the matrix (Figures 4 and 5(c)).

With prolonged annealing time at the upquenching temperature, the droplets will shrink in size as Mg and Si diffuse away from the droplets into the surrounding matrix. During this diffusion reaction, the chemical composition of the droplets is free to slide on the liquidus surface along the upquenching temperature isotherm, as shown in Figure 10. This is exactly what happens, because the rates of diffusion of the two alloying elements in the Al matrix are different (Figures 6(a)

through (d)). Since the $\beta$-phase particle is now absent, the melt is in equilibrium only with the $\alpha$-Al interface composition. It is thus free to change its composition as shown in Figure 10 in equilibrium with a changing interface composition along the 600 °C isotherm on the solidus surface as given by the corresponding tie-lines. This is contrary to observations of the binary Al-4.2 wt pct Cu alloy,[5] where the droplets had very nearly the same chemical composition during the entire dissolution process. The observed variations in Cu content were due solely to nucleation problems and were not dependent on annealing time.

Figure 10 shows the solidification path of a droplet. The composition of the droplet immediately after complete melting of the $\beta$ phase at 600 °C (and after the gradients in the melt have evened out) is given by X. During dissolution at 600 °C, the chemical composition of the droplet moves along the 600 °C isotherm on the liquidus surface to position X′, where the specimen is quenched and the droplet solidifies. Metallographic observations show that the droplet becomes increasingly enriched in Si with increasing holding time before quenching; *i.e.*, the amount of ternary eutectic increases with increasing annealing time (Figures 6(a) through (d)). This means that the Mg atoms diffuse away from the droplet more rapidly than do the Si atoms.

On solidification of a droplet of composition X′, the $\alpha$-Al phase solidifies initially. This occurs by inward epitaxial growth of the surrounding $\alpha$-Al matrix. The composition of the liquid moves down toward the eutectic valley, and at point X″ $Mg_2Si$ starts to precipitate out together with the $\alpha$-Al phase as a binary eutectic. As seen in Figures 6(b) and (c), this binary eutectic has a fairly coarse appearance.

During this binary eutectic solidification process, the composition of the remaining liquid moves down the eutectic valley and finally reaches the ternary eutectic point, where the Al-$Mg_2Si$-Si ternary eutectic is formed. This eutectic has a rather fine structure, as shown in Figures 6(b) through (d).

When this ternary eutectic forms, some of the $Mg_2Si$ precipitation will initially occur on the $Mg_2Si$ particles that are part of the binary eutectic. However, when the ternary eutectic grows, the binary eutectic becomes enveloped and new $Mg_2Si$ particles must be nucleated. These appear as finely dispersed $Mg_2Si$ particles in the part of the droplet where the solidification process apparently is completed. Thus, after solidification the two eutectics appear as three eutectics—binary Al-$Mg_2Si$, binary Al-Si, and ternary Al-$Mg_2Si$-Si—due to nucleation problems of the different constituents.

The fine solidification structures of these eutectics hampered the attainment of good micrographs in the light microscope. Figure 11 shows an SEM micrograph of such a solidified droplet obtained by using atom number contrast. The different eutectics are indicated. Due to the small difference in atom numbers, good contrast was difficult to obtain even with this technique.

With prolonged annealing before quenching, the droplets become increasingly enriched in Si. If annealing time is long enough, as shown in Figure 10, the droplets may reach the ternary eutectic point directly upon solidification (*i.e.*, no binary Al-$Mg_2Si$ eutectic is formed), or may even reach the binary Al-Si eutectic valley first and then move to the ternary eutectic point. The resulting solidification structure, composed of $\alpha$-Al, Si, and $Mg_2Si$, may appear as a finely dispersed structure (Figure 6(d)).

2. $\alpha\text{-}Al + Mg_2Si \rightarrow liq$ *at* $T < T_{eut}$

The melting reaction at temperatures below the eutectic temperature will now be discussed. Figure 9 shows a solvus isotherm (dotted line) at a temperature below the eutectic temperature. The isotherm has been extended into the two-phase field. Immediately after

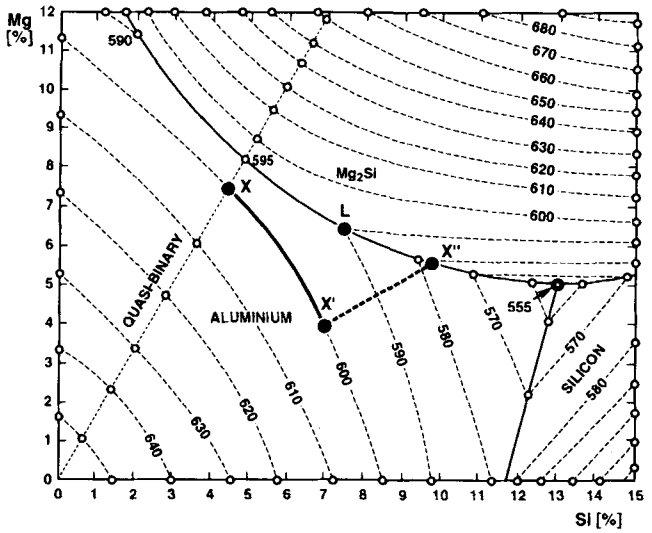


Fig. 10—Liquidus surface as given by Phillips.[7] Point X indicates the melt composition as the melting reaction is completed at 600 °C, X′ the change in composition after a certain dissolution time at 600 °C, and X″ the composition of the melt as the Al-$Mg_2Si$ eutectic starts to precipitate when the samples are quenched after this dissolution time. Point L shows the melt composition as the melting reaction is completed at 590 °C.

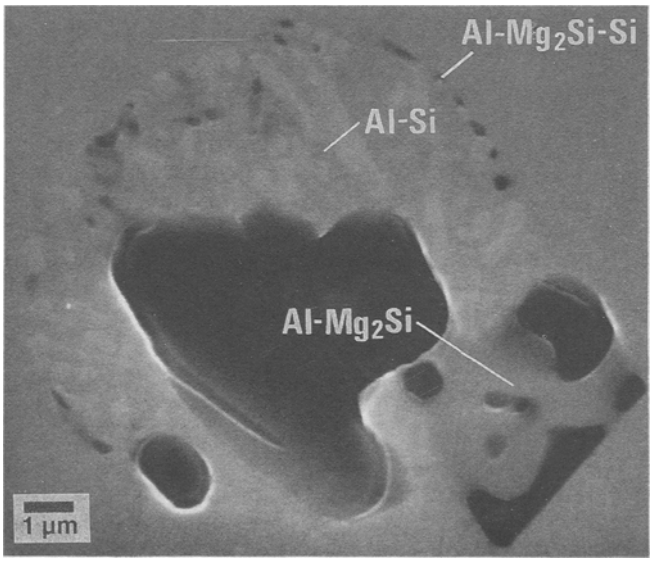


Fig. 11—SEM micrograph of a solidified droplet after annealing at 600 °C for 60 s before quenching. The three different eutectics resulting from nucleation problems of the different constituents are indicated. Alloy 2, melting reaction: Al + $Mg_2Si \rightarrow$ liq.

upquenching to this temperature, the interface concentration will be located at point Y on this isotherm, defined by Eq. [A6] During dissolution of the $\beta$-$Mg_2Si$ particle, this point is not fixed, but slides along the isotherm toward the limiting concentration Z given by Eq. [A7] which is obtained after long dissolution times. If Y is in the $\alpha$ field and Z is in the two-phase field ($\alpha$ + liquid), the condition for local melting is satisfied when the interface concentration crosses the line for the maximum extension of the $\alpha$ field.

This explains the observation that local melting of the $Mg_2Si$-phase particles may occur at a temperature below the eutectic temperature, and that some time is needed at this temperature before melting starts. (At 590 °C, the first sign of a eutectic in connection with the $Mg_2Si$ particles was evident after an annealing time of approximately 20 to 40 seconds.)

Figure 12(a) shows an isothermal section of the Al-Mg-Si phase diagram at 590 °C as given by Phillips,[7] and Figure 12(b) shows an enlarged portion of the Al corner of this section. The line between points $\alpha_1$ and $\alpha_2$ in Figure 12(b) is the 590 °C isotherm on the solvus surface, which has been extended into the two-phase field to a point called $\alpha_3$ (dotted line). The line between point $\alpha_2$ and the binary Al-Si axis is the 590 °C isotherm on the solidus surface. Points Y and Z are equivalent to points Y and Z in Figure 9.

Figure 12(a) shows that at 590 °C an equilibrium situation may exist between $\alpha$-Al phase of composition $\alpha_2$, liquid of composition L, and $\beta$-$Mg_2Si$. It is clearly seen that the composition of the melt in this case is no longer located on (or close to) a straight line between the two solid phases. This means that the melt composition, L, cannot be obtained simply by melting $\alpha$ phase and $\beta$ phase in the correct proportions. The melt composition will in this case be adjusted by diffusion of Mg and Si atoms into the $\alpha$-Al phase. The melting reaction will thus be controlled by diffusion in the $\alpha$ phase, and this explains why the melting reaction takes some time at temperatures below the eutectic temperature, whereas it occurs nearly spontaneously above the eutectic temperature. In fact, complete melting of $Mg_2Si$-phase particles in alloy 2 was not observed until ~2-minute annealing time at 590 °C.

In order to be able to create a melt, it is anticipated that the $\alpha$-Al interface composition must be located somewhat beyond point $\alpha_2$ along the solvus isotherm—for example, at point $\alpha_3$ in Figure 12(b). After a melt has been nucleated, a gradient in the melt will be established.

If $D^{liq}_{Mg} > D^{liq}_{Si}$, the gradient of Mg will be smaller than two times the gradient of Si, as indicated by Figure 12(a). When melting has started, the $\alpha$-Al composition in equilibrium with the melt will be located on the solidus isotherm, as indicated by point S in Figure 12(b). The location of this point in equilibrium with melt of composition $L_\alpha$ is then given by the corresponding tie-line, as indicated in Figure 12(a). Figure 12(a) also shows the tie-line connecting the liquid composition $L_\beta$ in equilibrium with the $\beta$-$Mg_2Si$-phase particle. The indicated gradient in the melt is considered necessary for the reaction to occur. As the melting reaction in this case is controlled by diffusion in the solid

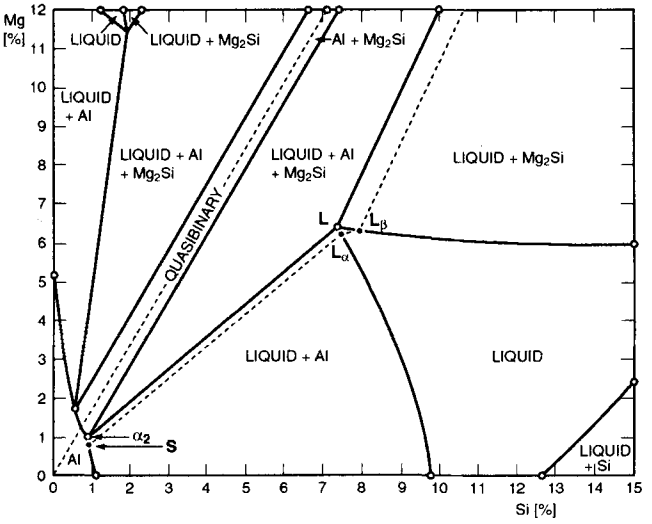


(a)

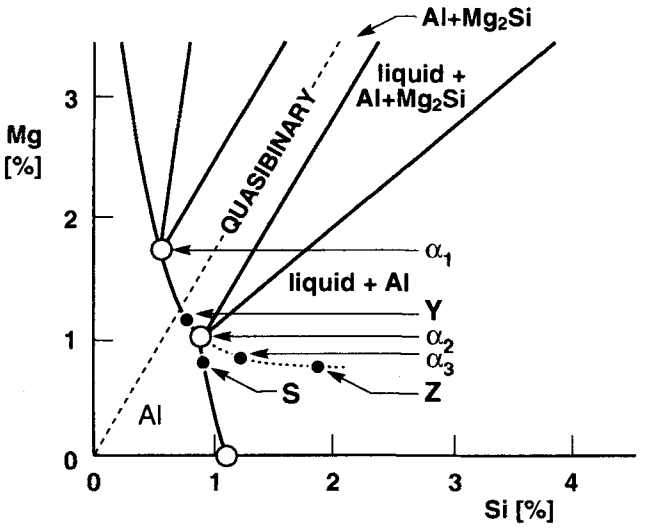


(b)

Fig. 12—Isothermal section of the Al-Mg-Si phase diagram at 590 °C as given by Phillips.[7] (*b*) is an enlarged portion of the Al corner in (*a*). Points $\alpha_1$, $\alpha_2$, $\alpha_3$, S, L, $L_\alpha$, and $L_\beta$ are schematically indicated (see text).

$\alpha$ phase, this gradient in the melt must, however, be very small and has for reasons of clarity been exaggerated in Figure 12.

The solidification path for the melt in the case of $T < T_{eut}$ is quite similar to the one described previously for melting at 600 °C ($T > T_{eut}$). As long as the $\beta$-$Mg_2Si$-phase particle exists, the composition of the melt will be approximately constant and located at (or close to) point L in Figure 10. When the samples are quenched, the composition of the liquid moves down the eutectic valley and $Mg_2Si$, together with the $\alpha$ phase, solidifies. This occurs by epitaxial growth of both the surrounding matrix and the still-remaining $\beta$-$Mg_2Si$ phase. As the remaining liquid finally reaches the ternary eutectic point, the ternary Al-$Mg_2Si$-Si eutectic is formed.

At short dissolution times when the volume of the melt is small, most of the $Mg_2Si$ in this ternary eutectic

solidifies on the existing $Mg_2Si$ particle, and the ternary eutectic appears as a binary Al-Si eutectic (Figure 7(b)). When the volume of the ternary eutectic becomes larger, new precipitation of $Mg_2Si$ takes place, quite analogous to the situation shown in Figure 11.

During dissolution, but before melting starts, the $Mg_2Si$ particles seem to have a well-rounded shape (see Figure 7(a)). The faceted shape of the $Mg_2Si$ phases shown in Figures 7(b) and (c) is probably due to the anisotropic growth of a $Mg_2Si$ crystal into the surrounding melt. Exactly when melting starts at 590 °C is difficult to determine. The volume fraction of the ternary eutectic is low and thus difficult to detect. The eutectic liquid, when small enough, may be consumed by the existing $Mg_2Si$ and a supersaturated $\alpha$ phase due to problems in nucleating Si during solidification. (In some cases, only a single Si particle was observed in connection to an $Mg_2Si$ particle.) The faceted shape of the $Mg_2Si$ phase particles, however, was observed at somewhat shorter annealing times than the first appearance of the eutectic. This may indicate that local melting has taken place, even though the well-developed eutectic is not found after subsequent cooling.

When the entire $Mg_2Si$-phase particle has melted and the droplet is dissolving into the $\alpha$-Al matrix, the melt is free to change its composition along the 590 °C liquidus isotherm, as previously discussed for melting at 600 °C (Figure 10). The situation is now identical to the previous one, where the droplets after solidification show a decreasing amount of the binary Al-$Mg_2Si$ eutectic and an increasing amount of ternary eutectic. At long enough dissolution times before quenching, only ternary or even binary Al-Si plus ternary eutectic may form (Figure 7(e)).

The samples of alloy 2 that were equilibrated at 500 °C also had to be upquenched to 593 °C in order for the melting reaction to be completed after ~0 second annealing time ($\alpha$-Al + $Mg_2Si \rightarrow$ liq). In this case, the $\alpha$-Al concentration is somewhat to the right of the quasi-binary composition (Figure 8), and it should therefore be possible to identify a temperature lower than the eutectic temperature above which all three phases—$\alpha$-Al, liquid, and $\beta$-$Mg_2Si$—are located along a straight line in the phase diagram. In such a situation this melting reaction should also be expected to occur nearly spontaneously at temperatures below the quasi-binary eutectic temperature. This was not detected in the samples upquenched to 592 °C, a probable indication that the eutectic Al-$Mg_2Si$ valley is rather flat close to the quasi-binary point. In this case the three phases are not located along a straight line in the diagram even at 592 °C, and the situation is analogous to that described for melting at $T < T_{eut}$.

In order for the melting reaction to take place spontaneously at lower than the quasi-binary eutectic temperature, the upquenching temperature would therefore have to be adjusted on a finer scale between 592 °C and 593 °C. However, in the samples that had been upquenched to 593 °C with ~0 second annealing time, some ternary eutectic was observed in addition to the binary Al-$Mg_2Si$ eutectic in the solidified droplets. This indicates that the average composition of the melt in these samples is somewhat to the Si side of the quasi-binary composition, which is to be expected as the $\alpha$-Al composition is also to the Si side.

Another point of interest related to the samples of alloy 2 equilibrated at 500 °C is that the first sign of a eutectic in connection with the $Mg_2Si$-phase particles was detected after ~0 second annealing time at 590 °C, whereas this was not observed until annealing had taken place for about 20 to 40 seconds at 590 °C in samples of the same alloy equilibrated at the lower temperature. The probable reason for this is that the point described by Eq. [A6] is located in the two-phase field for the samples equilibrated at 500 °C and is in the $\alpha$-Al field for the samples equilibrated at the lower temperature. (According to Eq. [A6], $\Delta Mg/\Delta Si$ is the same, but the $\alpha$-Al composition before upquenching is located farther to the right in the samples equilibrated at 500 °C, causing point Y in Figure 9 to be located in the two-phase field.) Upquenching the samples equilibrated at 500 °C to 590 °C will thus immediately give an interphase composition that is within the two-phase field.

According to the phase diagram, melting of secondary $Mg_2Si$-phase particles at $T < T_{eut}$ should be possible at all temperatures down to the ternary eutectic temperature. In practice, the difference between $D^{\alpha}_{Mg}$ and $D^{\alpha}_{Si}$ determines whether or not the point described by Eq. [A7] moves into the two-phase field at the temperature considered. (In alloy 2, melting of $Mg_2Si$ was observed at 580 °C after an annealing time of 8 minutes.)

Also of interest is that, according to Eq. [A5], the smaller the dissolving particle, the more quickly will the point described by Eq. [A7] be approached. This means that melting should first appear in connection with small particles. However, it was not possible to verify the prediction in this investigation. One problem is that the liquid droplet may be so small that the resulting eutectic after solidification consists of only one $\alpha$-phase particle and one $\beta$-phase particle. The $\alpha$ phase will then be difficult to distinguish from the Al matrix, and, under microscopic examination, the eutectic structure may appear as only one $\beta$-phase particle, thus making it difficult to determine whether melting has actually taken place.

### B. *$\alpha$-Al + Si → liq (Alloy 2)*

Another melting reaction found in alloy 2 was the reaction between the free Si-phase particles and the surrounding $\alpha$-Al matrix, as shown in Figure 5(b). This is the same reaction as that observed in an Al-1.2 wt pct Si alloy by Lohne and Ryum,[4] and the situation is analogous to the melting reaction in an Al-4.2 wt pct Cu alloy described by Reiso *et al.*[5] The only difference from the reaction in a binary alloy may be that, if the alloy has not been brought to equilibrium at a low enough temperature before upquenching, the matrix composition around the Si-phase particle will differ slightly from the corresponding concentration in the binary Al-Si alloy.

If this is the case, the resulting matrix composition in equilibrium with the Si-phase particle after upquenching may be such that melting is possible below the Al-Si binary eutectic temperature of 577 °C, as given in

Reference 7. Because the free Si-phase particles in alloy 2 were rather scarce and difficult to detect, the exact melting temperature for this reaction was difficult to determine. However, the reaction was observed in the samples upquenched to 573 °C with ~0 second annealing time, *i.e.*, well below the binary Al-Si eutectic temperature of 577 °C.

When this melting reaction occurs at temperatures below the Al-Si eutectic temperature, a small amount of the ternary Al-$Mg_2Si$-Si eutectic should also be expected to be present in connection with the binary Al-Si eutectic in the solidified droplets. This was in fact verified by metallographic examination of these samples [An appearance similar to that shown in Figure 13(d) (*vide infra*)].

### C. $\alpha$-Al + $Mg_2Si$ + Si → liq (Alloy 2)

The third melting reaction found in alloy 2 was the reaction between $\alpha$-Al, $Mg_2Si$, and Si-phase particles, with all the phases in physical contact with one another (Figure 2(b)). After upquenching to 560 °C (~0-second annealing time), this agglomerate melted and formed a very fine ternary eutectic upon subsequent solidification (Figure 5(a)).

When this structure is upquenched from the low-temperature equilibrium condition, the matrix in contact with both the $Mg_2Si$ and the Si-phase particles has only one possible equilibrium composition. This interface must be in equilibrium with both of these phases—a state obtained when the interface concentration follows the line described by the apex of the three-phase field $\alpha$-Al + $Mg_2Si$ + Si (Figure 8). As this interface concentration reaches the eutectic composition (moves into a liquid field), the condition for melting is satisfied and eutectic melting occurs. This ternary eutectic temperature is the lowest temperature at which a melt can exist in this system, and thus local melting of secondary phases should not be possible below this temperature.

The temperature at which this ternary reaction occurred was studied by annealing individual samples at 1 °C intervals from 555 °C to 560 °C, with annealing times of up to 60 seconds at each temperature. The temperature had to be increased to 560 °C before the reaction started, and at this temperature the reaction was very rapid, with complete melting after ~0 second annealing time. These results suggest a ternary eutectic temperature of 559 °C, as given in *Metals Handbook*,[8] rather than 555 °C, as given by Phillips,[7] (The temperature must be slightly above the eutectic temperature for the reaction to occur.)

From Figure 10 it can be seen that at (or just slightly above) the ternary eutectic temperature the composition of the melt is restricted to the ternary eutectic composition. If the size of the $Mg_2Si$ and Si particles are such that one gets a surplus of one type of the particles with respect to what is necessary to create the ternary eutectic composition, the appearance of the ternary eutectic after solidification will differ. Figure 13(a) shows a fine ternary eutectic resulting from complete melting of the Si-phase particle and a corresponding amount of melted $Mg_2Si$ and $\alpha$-Al, and the unreacted remnant of the $Mg_2Si$ particle. Figure 13(b) shows a much coarser ternary eutectic together with unreacted Si resulting from a surplus of an Si-phase particle.

At temperatures markedly above the ternary eutectic temperature, the composition of the melt may vary considerably (Figure 10). As the temperature is increased, the surplus particles may also melt completely, and the resulting structures after subsequent solidification will in principle be the same as those previously discussed after complete melting at 600 °C and 590 °C. Figure 13(c) shows the structure after melting at 577 °C with a surplus of $Mg_2Si$. Upon solidification, precipitation of the rather coarse quasi-binary $\alpha$-Al + $Mg_2Si$ eutectic appears first, followed by a very fine ternary eutectic as the melt composition finally reaches the ternary eutectic point. Figure 13(d) shows the corresponding situation with a surplus of Si. Solidification of the liquid droplet in this case first causes precipitation of a rather coarse binary Al-Si eutectic and then a rather coarse ternary eutectic.

The different appearances of the ternary eutectic in these situations can most likely be attributed to the nucleation conditions of the different constituents. If unreacted Si is still present, or if the melt is rich in Si so that Al-Si eutectic is precipitated first during solidification, the ternary eutectic will have a rather coarse appearance. If Si is not nucleated until the ternary eutectic solidifies, it will have a much finer appearance.

## V. CONCLUSIONS

1. Microstructural observations of local melting of secondary phases in two ternary Al-Mg-Si alloys with mean compositions well below the maximum solid-solubility composition have been presented. In the quasi-binary alloy, one melting reaction was found

   $$\alpha\text{-Al} + Mg_2Si \rightarrow \text{liq}$$

   whereas in the alloy with excess Si concentration, three reactions occurred

   $$\alpha\text{-Al} + Mg_2Si \rightarrow \text{liq (the same reaction as above)} \quad [1]$$

   $$\alpha\text{-Al} + Si \rightarrow \text{liq} \quad [2]$$

   $$\alpha\text{-Al} + Mg_2Si + Si \rightarrow \text{liq} \quad [3]$$
2. Reaction [1] occurs at temperatures both above and below the quasi-binary eutectic temperature.
3. The interface concentration determines when melting is possible. In these ternary alloys, this interface composition cannot be determined from the phase diagram alone; the rate of diffusion of Mg and Si also must be taken into account. This explains why melting of $Mg_2Si$ is possible below the quasi-binary eutectic temperature. The results can only be explained by assuming that $D_{Mg} > D_{Si}$ at the temperatures investigated.
4. The time needed for complete melting is very short for all three reactions when the upquenching temperature exceeds the respective eutectic temperature. It is anticipated that the reaction rates in these cases are controlled by diffusion of the alloying elements in the liquid.
5. At $T < T_{eut}$, complete melting for reaction [1] may require a substantial period of time, and in samples

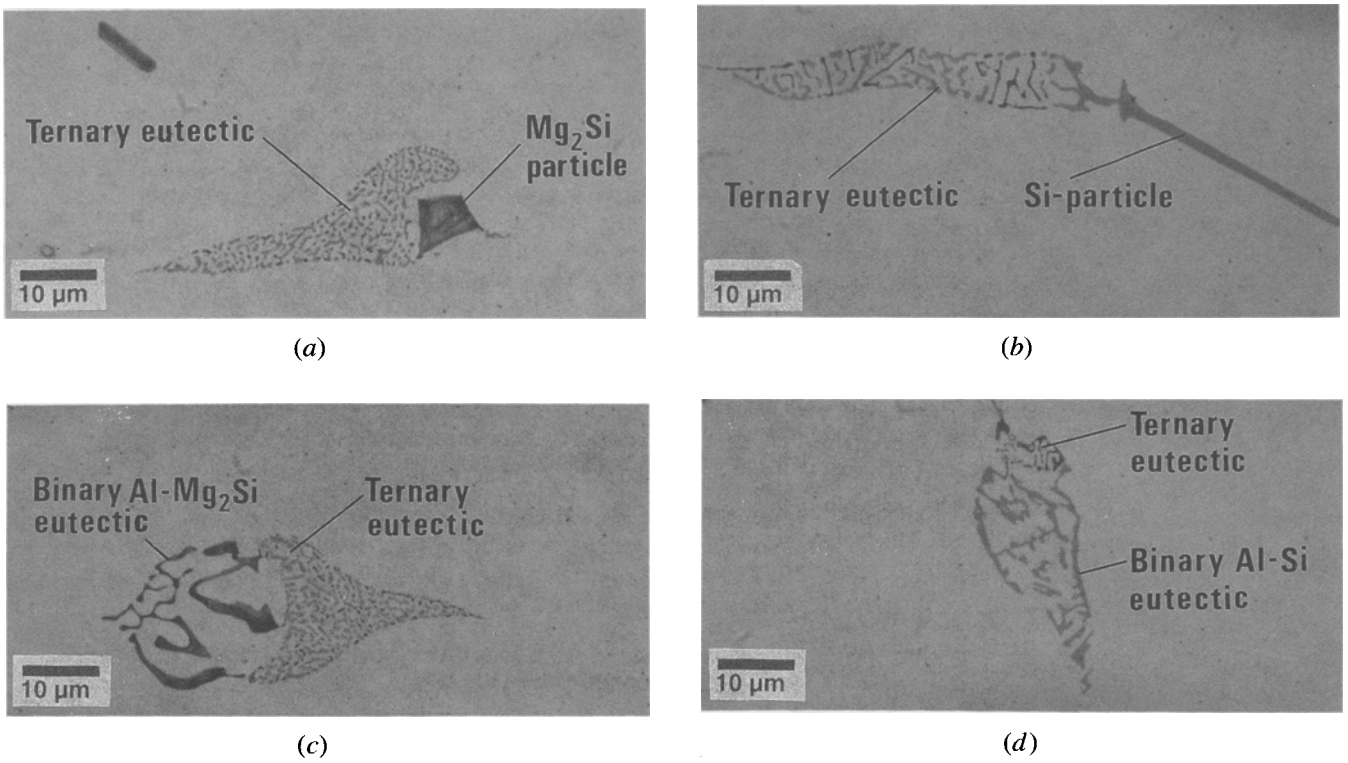


Fig. 13—Different appearances of the ternary eutectic after solidification (alloy 2, light microscopy): (*a*) and (*b*) show the structure after upquenching to 560 °C (~0 s annealing time) before cooling, with an unreacted remnant from a surplus of an $Mg_2Si$ particle (a) and a surplus of an Si particle (b); (*c*) and (*d*) show the resulting structures after upquenching to 577 °C (~0 s annealing time) with a surplus of $Mg_2Si$ (c) and Si (d), where the surplus particles are completely melted prior to cooling.

equilibrated at a low temperature before upquenching, melting was not initiated until after a certain period of annealing. The reaction rate in this case is assumed to be controlled by diffusion of the alloying elements in the solid $\alpha$-Al phase.

6. The composition of a droplet is found to change with increasing annealing time after melting is complete.
7. The resulting eutectic structure after quenching of a droplet is explained by the phase diagram in conjunction with the nucleation conditions of the constituents involved.
8. The ternary eutectic temperature of 559 °C, as given in *Metals Handbook*,[8] is in better agreement with the observed results than 555 °C, as given by Phillips.[7] Likewise, a quasi-binary eutectic temperature of 593 °C, as given by Fischer,[11] fits the current results better than 595 °C, as given by Phillips[7] and *Metals Handbook*.[8]

## APPENDIX

In this appendix, a calculation is carried out of the kinetics of the dissolution of a spherical $\beta$-$Mg_2Si$ particle at temperature $T$ after upquenching from a lower temperature at which equilibrium has been obtained. It is assumed that the rate of dissolution is limited by volume diffusion.

The equations to be solved are the two Fick's equations for diffusion of Mg and Si atoms. It is also assumed that the $\beta$ phase is very close to the composition $Mg_2Si$ at all temperatures so that no diffusion occurs within this phase. Finally, it is assumed that there is no interaction between Mg and Si atoms during diffusion. The following two equations for diffusion in the $\alpha$ phase result:

$$\frac{\partial C_j}{\partial t} = D_j^\alpha \left[ \frac{\partial^2 C_j}{\partial r^2} + \left(\frac{1}{r}\right)\left(\frac{\partial C_j}{\partial r}\right) \right] \qquad (j = Mg, Si) \qquad [A1]$$

The boundary conditions are

$$\frac{dr^*}{dt} = \frac{D_j^\alpha}{(C_j^\beta - C_j^i)} \left(\frac{\partial C_j}{\partial r}\right)_{r=r^*} \qquad (j = Mg, Si) \qquad [A2]$$

where $r^*$ is the position of the phase boundary $\beta/\alpha$ and is equal to the size of the $\beta$-phase particle, $C_j^\beta$ is the concentration within this particle, $C_j^i$ is the interface composition, and $D_j^\alpha$ is the diffusion coefficient.

The stationary interface approximation[13] is now applied to Eqs. [A1] and [A2], which implies that $(\partial C_j/\partial r)_{r=r^*}$ is independent of the velocity $dr^*/dt$ of the interface and also independent of the curvature of the particle. The solutions to Eq. [A1] are[10]

$$C_j = C_j^\infty + \frac{(C_j^i - C_j^\infty)_{r^*}}{r}\left(1 - \text{erf}\frac{r - r^*}{2\sqrt{D_j^\alpha t}}\right) \qquad (j = Mg, Si) \qquad [A3]$$

where $C_j^\infty$ is the concentration remote from the $\beta$-phase particle. From Eq. [A3], $(\partial C_j/\partial r)_{r=r^*}$ is found and combined with Eq. [A2] to give the following two equations:

$$\frac{dr^*}{dt} = \frac{-k_j}{2}\left(\frac{D_j^\alpha}{r^*} + \sqrt{\frac{D_j^\alpha}{\pi t}}\right) \qquad (j = Mg, Si) \quad [A4]$$

where

$$k_j = 2\left(\frac{C_j^i - C_j^\infty}{C_j^\beta - C_j^i}\right) \cong 2\left(\frac{C_j^i - C_j^\infty}{C_j^\beta}\right)$$

Combining the two equations that Eq. [A4] gives, as

$$\left[\frac{dr^*}{dt}\right]_{Mg} = \left[\frac{dr^*}{dt}\right]_{Si}$$

yields

$$\frac{C_{Mg}^i - C_{Mg}^\infty}{C_{Si}^i - C_{Si}^\infty} = 2\left(\frac{\frac{D_{Si}^\alpha}{r^*} + \sqrt{\frac{D_{Si}^\alpha}{\pi t}}}{\frac{D_{Mg}^\alpha}{r^*} + \sqrt{\frac{D_{Mg}^\alpha}{\pi t}}}\right) \quad [A5]$$

where we have used $C_{Mg}^\beta/C_{Si}^\beta = 2$.

Two limiting cases are now discussed. For short dissolution times,

$$\frac{C_{Mg}^i - C_{Mg}^\infty}{C_{Si}^i - C_{Si}^\infty} = 2\sqrt{\frac{D_{Si}^\alpha}{D_{Mg}^\alpha}} \quad [A6]$$

For long dissolution times,

$$\frac{C_{Mg}^i - C_{Mg}^\infty}{C_{Si}^i - C_{Si}^\infty} = 2\left(\frac{D_{Si}^\alpha}{D_{Mg}^\alpha}\right) \quad [A7]$$

From Eqs. [A6] and [A7] it is seen that when $D_{Si}^\alpha = D_{Mg}^\alpha$, the concentrations on the $\alpha/\beta$ interface after upquenching will remain in the quasi-binary section of the ternary diagram for all dissolution times. However, as shown in this investigation, when a liquid droplet is dissolving in the $\alpha$ matrix, the chemical composition of the droplet changes with dissolution time. The change is such that it can only be explained by assuming $D_{Mg}^\alpha > D_{Si}^\alpha$. Data in the literature give the same ranking of the diffusion coefficients.[12] This implies that on upquenching, the interface concentration will move to the Si side of the quasi-binary section. Immediately after upquenching, it will be in the point defined by Eq. [A6] and will then continue to move to the right along the isotherm toward the point defined by Eq. [A7]. If this point lies within the liquid field, the $\beta$ particle, together with the surrounding $\alpha$ matrix, will melt. This is exactly the kinetics shown qualitatively in Figure 7.

## ACKNOWLEDGMENTS

The authors are grateful to Hydro Aluminum a.s for permission to publish this work. Many thanks are due to Hilde-Gunn Øverlie, Research Metallurgist, for assistance with experimental work and to Ulf Tundal, Ph.D. student, for valuable discussions, as well as to Terje Ustad, Senior Research Metallurgist, who performed the SEM analysis.

## REFERENCES

1. O. Reiso: *Proc. 3rd Int. Aluminum Extrusion Technology Seminar*, Aluminum Association, Washington, DC, 1984, vol. 1, pp. 31-40.
2. O. Reiso: *Proc. 4th Int. Aluminum Extrusion Technology Seminar*, Aluminum Association, Washington, DC, 1988, vol. 2, pp. 287-95.
3. H. Gjestland, A.L. Dons, O. Lohne, and O. Reiso: *Aluminum Alloys—Their Physical and Mechanical Properties*, Engineering Materials Advisory Service, Ltd., Warley, United Kingdom, 1986, vol. 1, pp. 359-70.
4. O. Lohne and N. Ryum: *Proc. 4th Int. Aluminum Extrusion Technology Seminar*, Aluminum Association, Washington, DC, 1988, vol. 2, pp. 303-08.
5. O. Reiso, H.G. Øverlie, and N. Ryum: *Metall. Trans. A*, 1990, vol. 21A, pp. 1689-95.
6. O. Reiso: *Strangpressen*, DGM, Oberursel, Germany, 1990, pp. 179-88.
7. H.W.L. Phillips: *Annotated Equilibrium Diagrams of Some Aluminium Alloy Systems*, The Institute of Metals, London, 1959, pp. 65-71.
8. *Metals Handbook*, 8th ed., ASM, Metals Park, OH, 1973, vol. 8, pp. 396-97.
9. D.E. Coates: *Metall. Trans.*, 1972, vol. 3, pp. 1203-12.
10. M.J. Whelan: *Met. Sci. J.*, 1969, vol. 3, pp. 95-97.
11. A. Fischer: Ph.D. Thesis, Technical University of Clausthal, Clausthal, Germany, 1976.
12. *Smithells Metals Reference Book*, 6th ed., Butterworth's, London, 1983.
13. H.B. Aaron, D. Feinstein, and G.R. Kotter: *J. Appl. Phys.*, 1970, vol. 41, p. 4404.